

Transient Diffusion in a Hygroscopic Bead

Presented to : Professor Phillip Servio

Prepared by

Ngan Jennifer Tram Su [260923530]

CHEE 390 – Computational Methods in Chemical Engineering

Department of Chemical Engineering

McGill University

2021.10.22

Table of Contents

Nomenclature.....	3
1 Objective.....	3
2 Flowchart	4
3 Results	5
4 Discussion.....	7
4.1 Effect of Biot and Fourier Number on Concentration Profile	7
4.2 Assumptions	7
4.2.1 First Term Approximation Assumption	7
4.2.2 Lumped Capacitance Assumption	8
4.3 Program Considerations	9
4.3.1 Bisection Method.....	9
4.3.2 Centerline Concentration	9
5 Conclusion	10
6 Appendix	11

Nomenclature

Bi_m	Biot Number
Fo_m	Fourier Number
θ_w^*	Dimensionless Concentration
G_n	Dimensionless Concentration Eigenvalue
r^*	Dimensionless Position

1 Objective

Desiccant beads dehumidify air by absorbing its moisture content. Once these beads reach saturation, they can be dried and reused. As the air's resident time in the fluidized bed increases, water slowly diffuses through the bead, creating a gradient that monotonically decreases towards the center. The objective of this report was to explore the effects of the Biot (Bi_m) and Fourier (Fo_m) numbers on the relationship between the bead's dimensionless concentration (θ_w^*) and position (r^*).

2 Flowchart

The implemented program prompts the user to enter a Biot number and a target centerline concentration. Figure 1 follows the path that these inputs follow to produce a 2D and 3D plot of the concentration profile, as well as the predicted time it takes for the centerline to reach the target concentration.

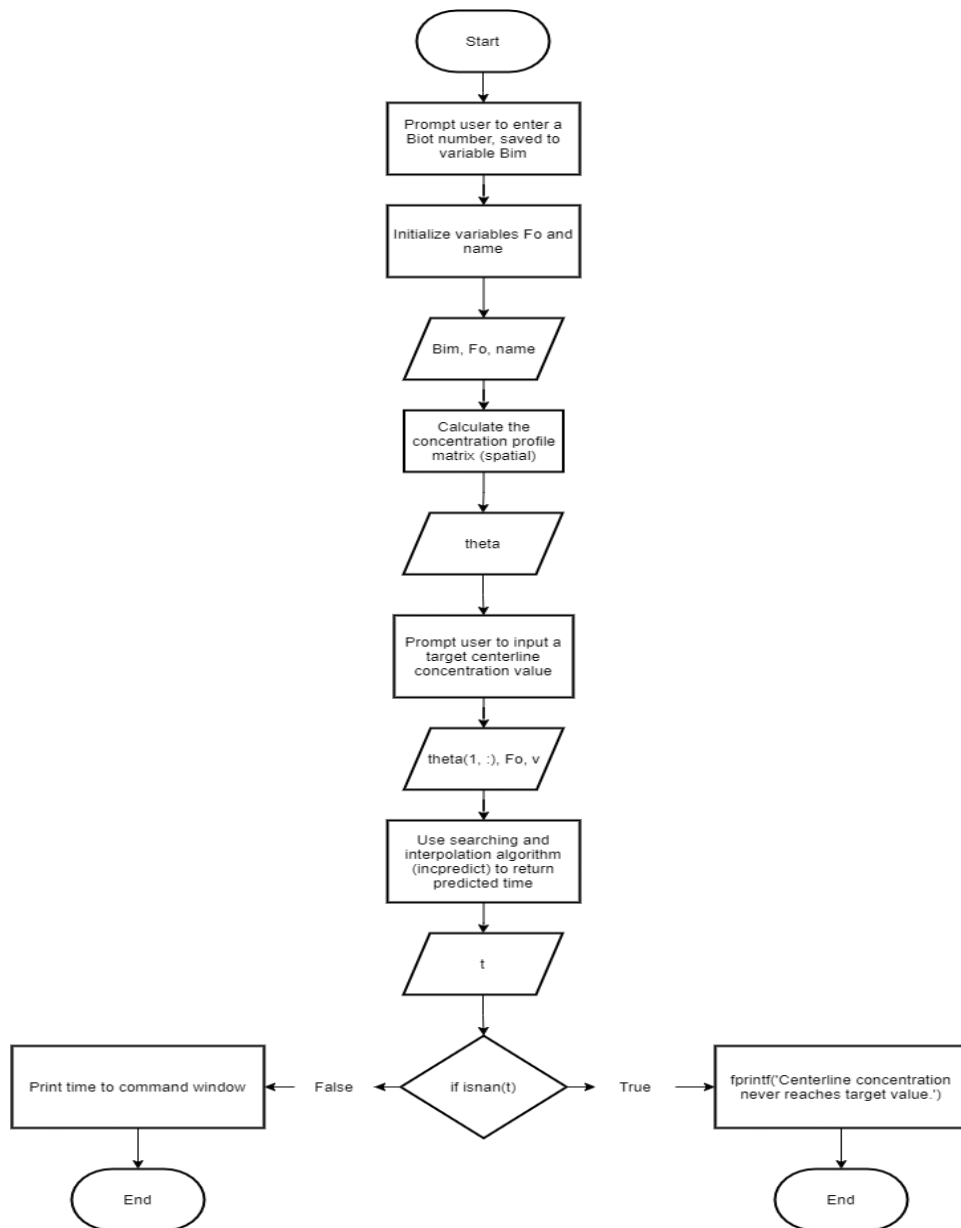


Figure 1 Main Program Flowchart

3 Results

The dimensionless concentration of a hygroscopic bead at a particular position and time is defined through equation (1). Its eigenvalues are defined through equation (2), whose independent variable consists of the positive roots of the transcendental equation (3).

$$\theta_w^* = 1 - \sum_{n=1}^{\infty} G_n \exp(-\zeta_n^2 F_{om}) \frac{1}{\zeta_n r^*} \sin(\zeta_n r^*) \quad (1)$$

$$G_n = \frac{4[\sin(\zeta_n) - \zeta_n \cos(\zeta_n)]}{2\zeta_n - \sin(2\zeta_n)} \quad (2)$$

$$0 = Bi_m - 1 + \zeta_n \cot(\zeta_n) \quad (3)$$

To determine the concentration profile of a hygroscopic bead, Brent's method was implemented as the root solver technique. These values were subsequently stored in a matrix of position (row) against time (column). Additionally, plots of concentration profiles with Fourier numbers ranging from (0, 2] and Biot numbers in the set {0.01, 0.1, 1, 10, 1000} were produced. Below are the plots (Figure 2, Figure 3) associated with a Biot number of 10 (and will continue to be the Biot number of interest for the remainder of the report). Plots for the remaining Biot numbers can be seen in the appendix.

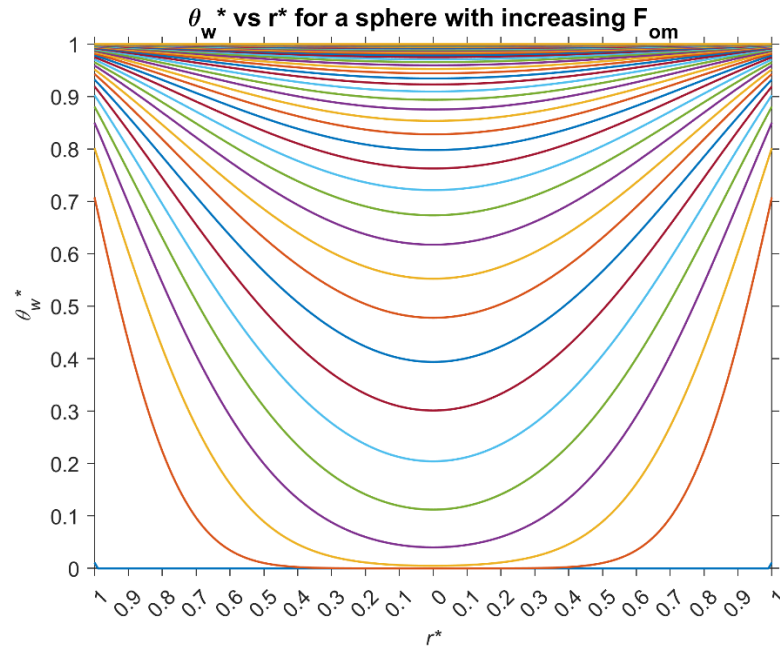


Figure 2 2D Concentration Profile of Water in a Spherical Bead with $Bi_m = 10$ and F_{om} ranging from $(0, 2]$

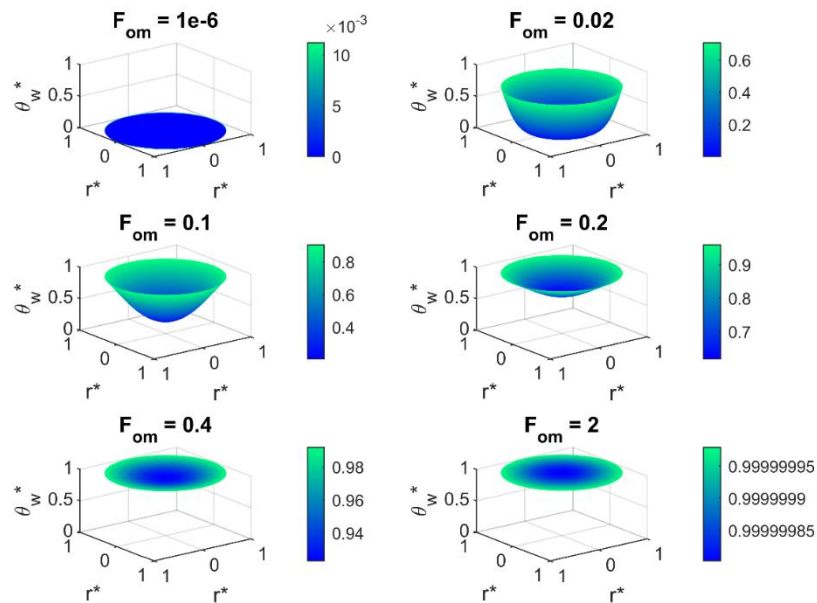


Figure 3 3D Concentration Profile of Water in a Spherical Bead with $Bim = 10$ and Fom ranging from $(0, 2]$

4 Discussion

4.1 Effect of Biot and Fourier Number on Concentration Profile

Concentration profiles across varying Biot and Fourier numbers can be found in the appendix. Low Biot numbers produce more uniform profiles, with concentrations remaining consistent and low over time. High Biot numbers demonstrate dependence on position, with concentrations reaching saturation as the Fourier number increases. As expected, all figures display a decreasing concentration as the position reaches the center; at high Fourier numbers, this saturation becomes more uniform throughout the sphere.

4.2 Assumptions

4.2.1 First Term Approximation Assumption

The first term approximation assumption states that the concentration profile can be adequately estimated by one eigenvalue when Fo_m is greater than 0.2. To validate this, the first term approximation was applied to all Fourier numbers and plotted (Figure 4).

Compared to Figure 2, it can be seen that the concentration profile is adequately approximated when a cut-off of 0.1 is applied to Fo_m (Figure 5). Similar conclusions can be

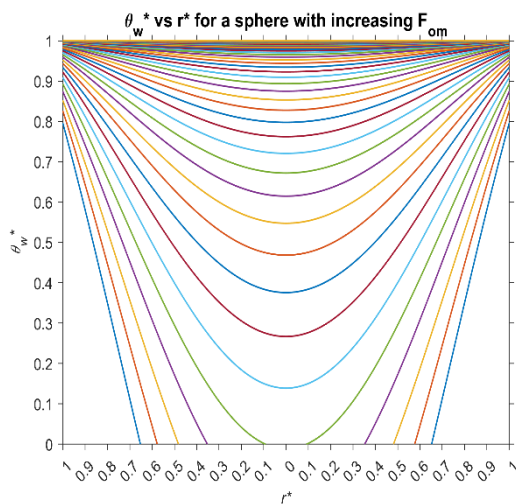


Figure 4 First Term Approximation for all Fourier Numbers at $Bi_m = 10$

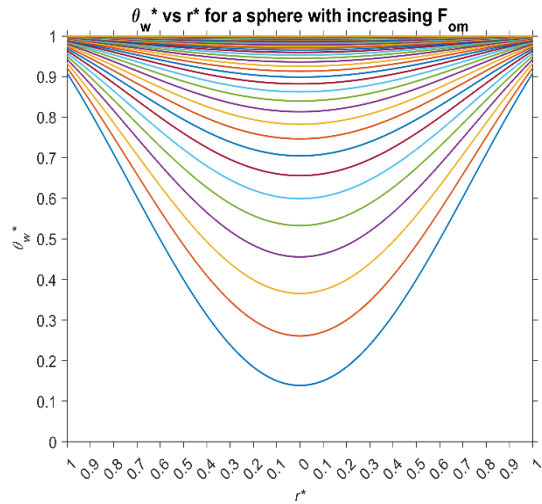


Figure 5 First Term Approximation Cut Off at $Fo_m = 0.1$ at $Bi_m = 10$

made with remaining Biot numbers. It can be observed that past this cut-off of 0.1, the general shape of the curve is maintained and does not cross the x-axis. However, as only one eigenvalue was calculated, the predicted concentrations in this approximation are lower than expected. As the cut-off is lower than the assumption's assertion of 0.2, the first term approximation is validated and is observed to hold true.

4.2.2 Lumped Capacitance Assumption

The lumped capacitance assumption states that the concentration profile is independent of spatial effects when the Biot number is less than 0.1. In other words, the concentration profile is uniform throughout the bead, regardless of time. Figure 6 depicts the concentration profile when the Biot number is set to 0.01, while Figure 7 uses a Biot number of 0.1.

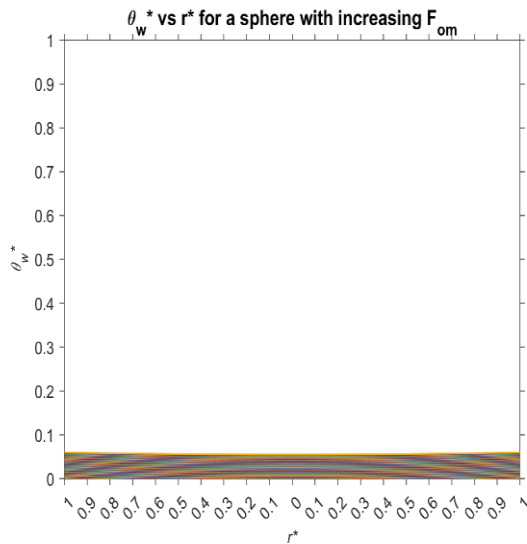


Figure 6 2D Concentration Profile of Water in a Spherical Bead with $Bi_m = 0.01$ and Fo_m ranging from $(0, 2]$

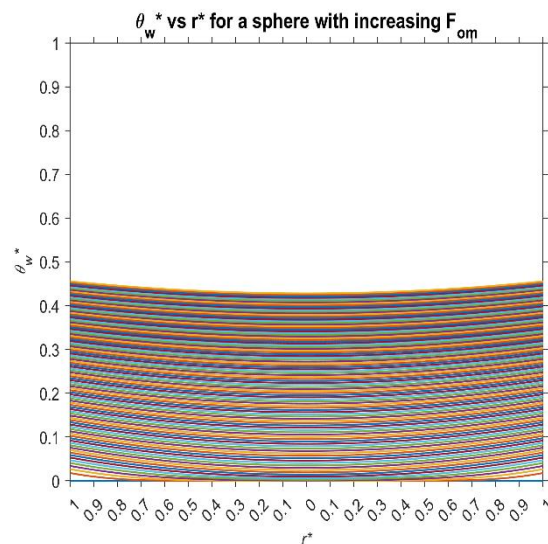


Figure 7 2D Concentration Profile of Water in a Spherical Bead with $Bi_m = 0.1$ and Fo_m ranging from $(0, 2]$

At 0.01, the concentration is low and uniform, with little to no curvature to indicate dependence on position. Reaching up to 0.1, some curvature begins to appear, thus indicating

the onset of positional dependence. Thus, the lumped capacitance assumption is observed to hold true.

4.3 Program Considerations

4.3.1 Bisection Method

The roots of the residual function (3) were found through Brent's method. However, as this algorithm fails in the vicinity of a singularity, this method was followed up by a more robust method – namely, the bisection method. Compared to other methods such as incremental search, bisection method is much faster as it halves the interval with each iteration. As well, bisection method is much more stable compared to methods such as linear interpolation, which fails when interpolating across a singularity.

4.3.2 Centerline Concentration

Equation (1) is undefined when r^* is zero (i.e. at the center of the sphere). Physically however, the concentration must be defined at that point, as water is slowly transferred to the center of the bead without hindrance. Through L'Hôpital's rule, the term $\frac{1}{\zeta_n r^*} \sin(\zeta_n r^*)$ can be represented as the limit as r^* approaches 0.

$$\lim_{x \rightarrow 0} \frac{\sin(ax)}{x} = a, a \in \mathbb{R}$$

Taking the limit over equation (1) will yield a defined value as the limit of products is the product of limits, thus defining a concentration as r^* approaches zero. While this value is mathematically defined, it is not recognized through MATLAB. To handle this calculation, the implemented program defines the range of r^* between eps and 1, where eps is a very small non-zero floating point value that acts as an approximation to zero.

5 Conclusion

Through Brent's root solving algorithm, the concentration profile of a hygroscopic bead was shown to greatly depend on position with increasing Biot numbers. At low Biot and Fourier numbers, the profile was uniform, while at high Biot numbers, the concentration decreased towards the center of the sphere, tending towards uniform saturation with increasing Fourier numbers. Thus, the first term approximation and lumped capacitance assumption were also shown to hold valid. Some considerations were also taken in the development of the program. Although Brent's method has fast convergence characteristics, it is unable to deal with singularities in the residual function. To compensate, the bisection method was implemented as a failsafe, doubling as a verification that a singularity was the cause of Brent's failure, as well as detecting any roots that Brent's may have missed. Finally, the undefined characteristic of equation (1) that arises when evaluated at $r^* = 0$ is managed by setting the left bound of r^* to ϵ .

6 Appendix

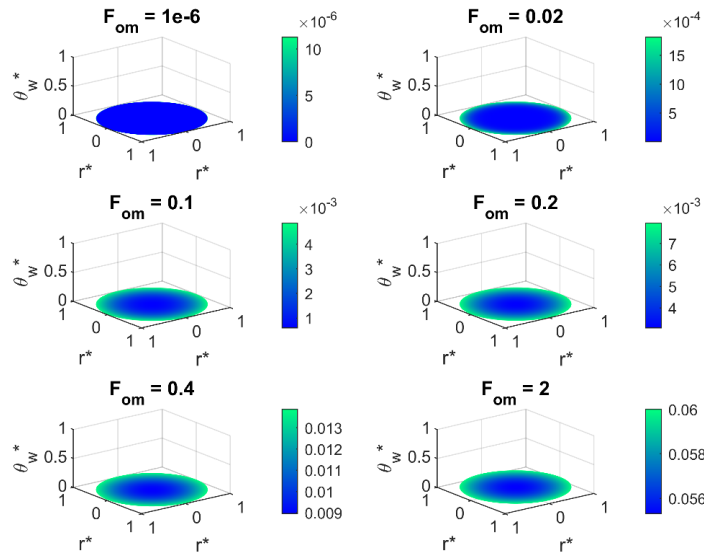


Figure 8 3D Concentration Profile of Water in a Spherical Bead with $Bi_m = 0.01$ and Fo_m ranging from $(0, 2]$

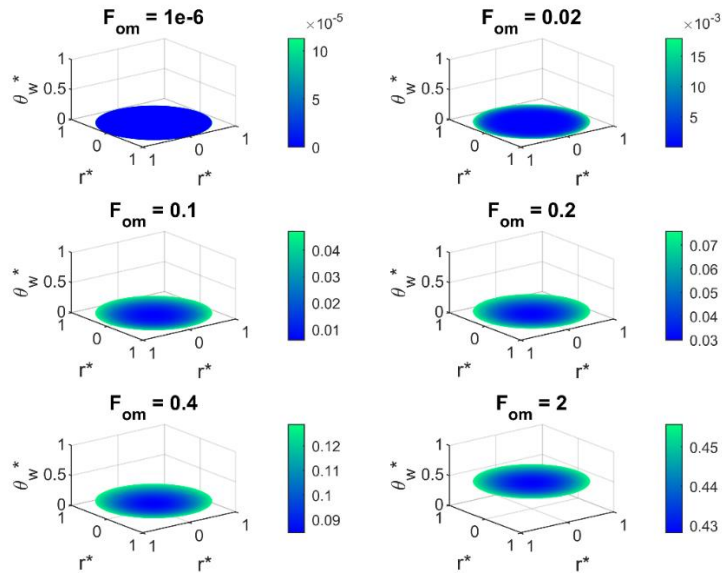


Figure 9 3D Concentration Profile of Water in a Spherical Bead with $Bi_m = 0.1$ and Fo_m ranging from $(0, 2]$

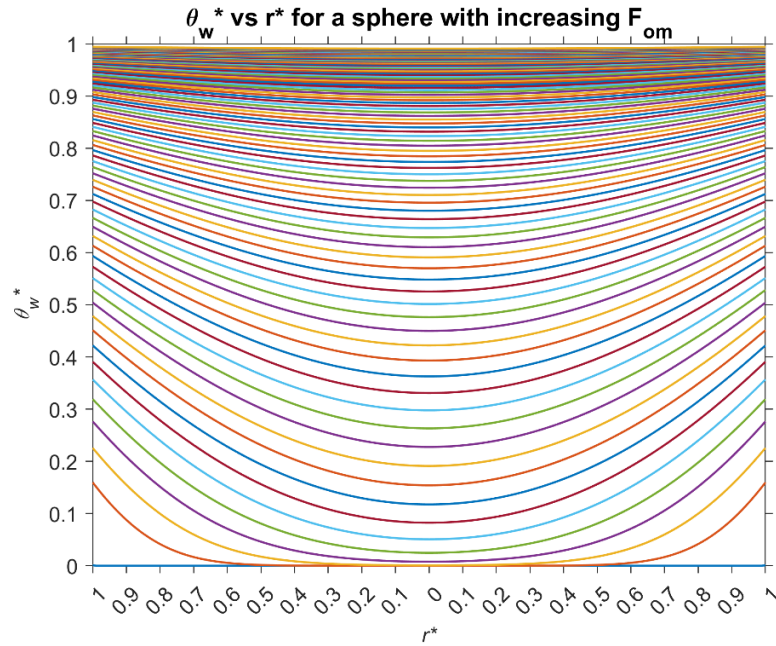


Figure 10 2D Concentration Profile of Water in a Spherical Bead with $Bi_m = 1$ and Fo_m ranging from $(0, 2]$

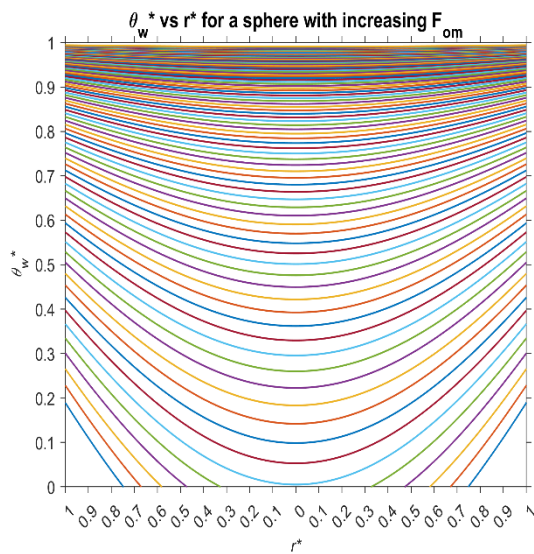


Figure 11 First Term Approximation for all Fourier Numbers at $Bi_m = 1$

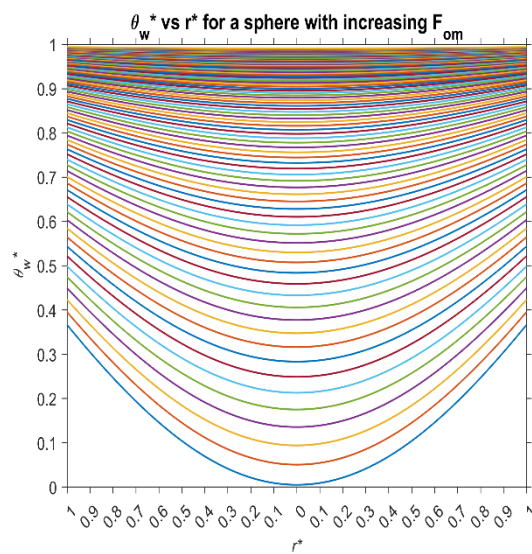


Figure 12 First Term Approximation Cut Off at $Fo_m = 0.1$ at $Bi_m = 1$

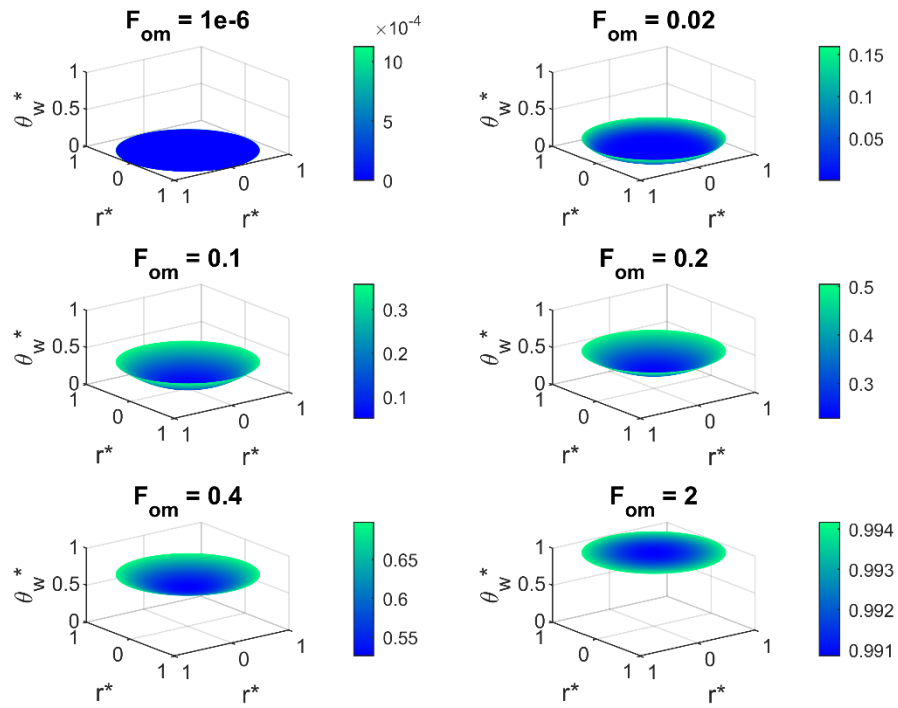


Figure 13 3D Concentration Profile of Water in a Spherical Bead with $Bi_m = 1$ and Fo_m ranging from $(0, 2]$

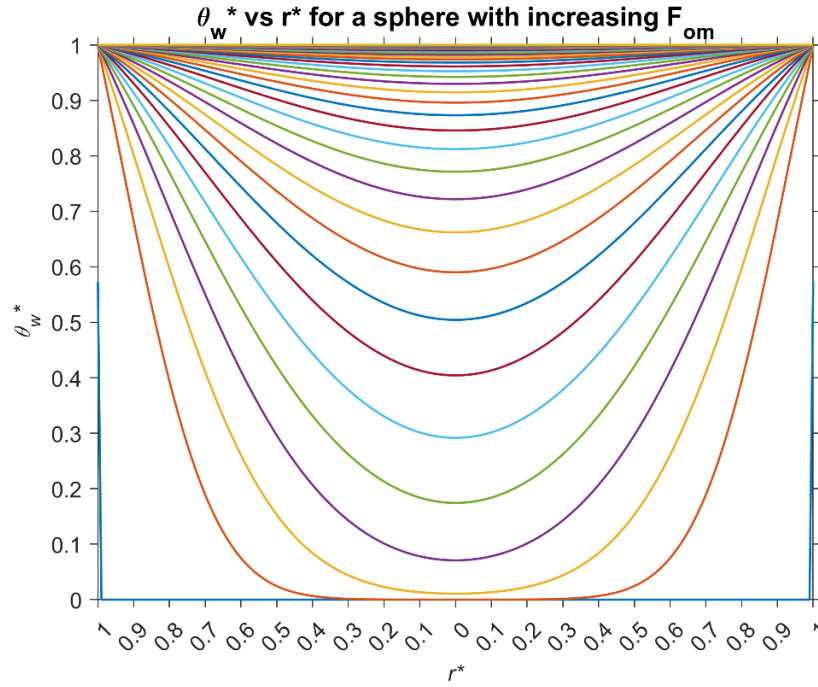


Figure 14 2D Concentration Profile of Water in a Spherical Bead with $Bi_m = 1000$ and F_{om} ranging from $(0, 2]$

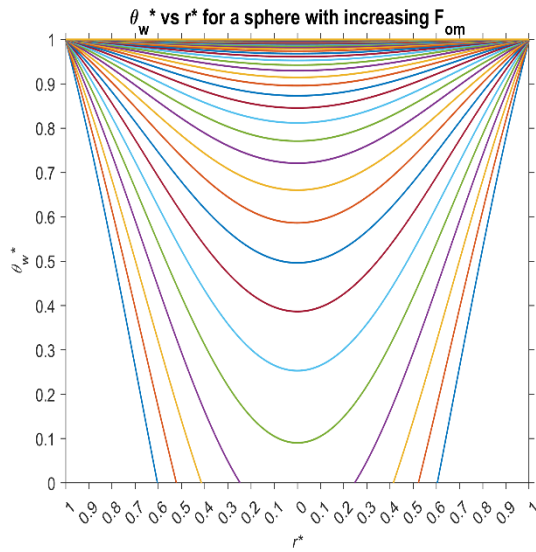


Figure 15 First Term Approximation for all Fourier Numbers at $Bi_m = 1000$

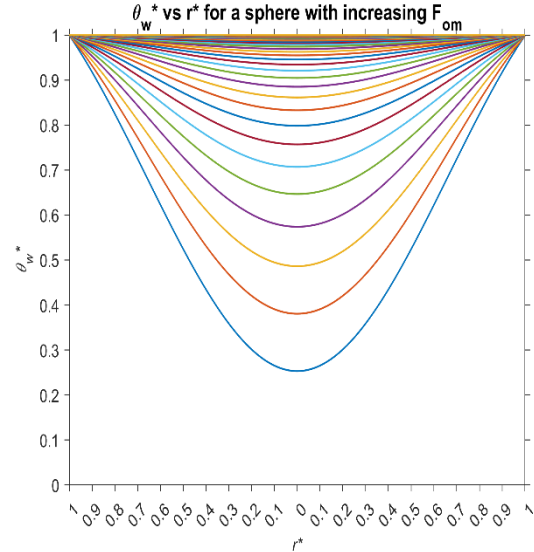


Figure 16 First Term Approximation Cut Off at $F_{om} = 0.1$ at $Bi_m = 1000$

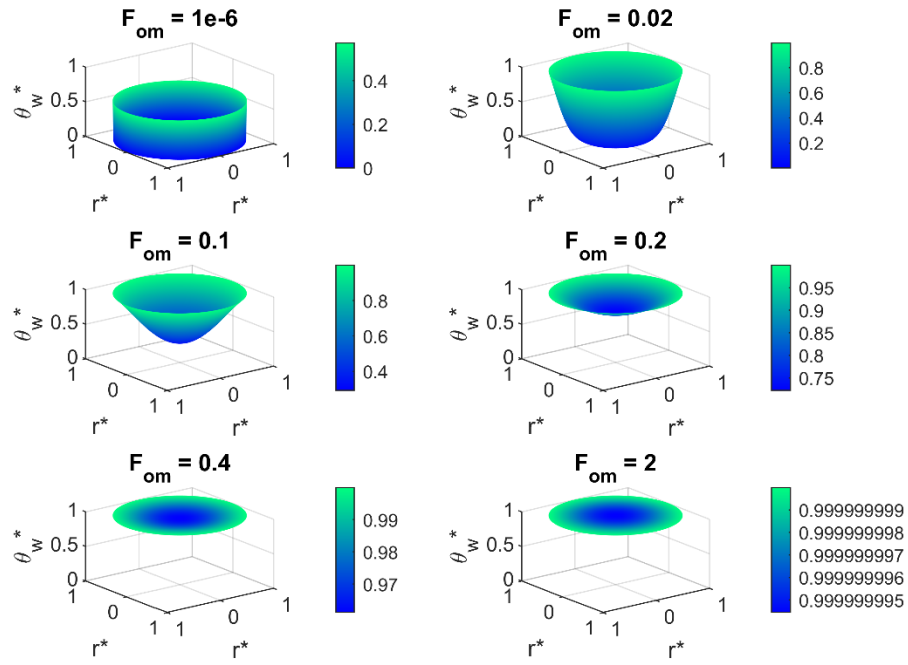


Figure 17 3D Concentration Profile of Water in a Spherical Bead with $Bi_m = 1000$ and Fo_m ranging from $(0, 2]$